Published in final edited form as:
Circ Res. 2009 February 27; 104(4): 531–540. doi:10.1161/CIRCRESAHA.108.188524.

ROCK Isoform Regulation of Myosin Phosphatase and Contractility in Vascular Smooth Muscle Cells

Yuepeng Wang[1], **Xiaoyu Rayne Zheng**[2], **Nadeene Riddick**[1], **Meredith Bryden**[1], **Wendy Baur**[1], **Xin Zhang**[2], and **Howard K. Surks**[1,*]

1 *Molecular Cardiology Research Institute and the Department of Medicine, Division of Cardiology, Tufts Medical Center*

2 *Laboratory for Microsystems Technology, Department of Manufacturing Engineering, Boston University*

Abstract

Abnormal VSMC contraction plays an important role in vascular diseases. The RhoA/ROCK signaling pathway is now well-recognized to mediate vascular smooth muscle contraction in response to vasoconstrictors by inhibiting myosin phosphatase (MLCP) activity and increasing myosin light chain (MLC) phosphorylation. Two ROCK isoforms, ROCK1 and ROCK2, are expressed in many tissues, yet the isoform specific roles of ROCK1 and ROCK2 in vascular smooth muscle (VSM) and the mechanism of ROCK-mediated regulation of MLCP are not well understood. In this study, ROCK2, but not ROCK1, bound directly to the myosin binding subunit (MBS) of MLCP, yet both ROCK isoforms regulated MLCP and MLC phosphorylation. Despite that both ROCK1 and ROCK2 regulated MLCP, the ROCK isoforms had distinct and opposing effects on VSMC morphology and ROCK2, but not ROCK1, had a predominant role in VSMC contractility. These data support that although the ROCK isoforms both regulate MLCP and MLC phosphorylation through different mechanisms, they have distinct roles in VSMC function.

Keywords

ROCK; myosin phosphatase; myosin light chain; myosin binding subunit

Introduction

Increased vascular tone plays an important role in the pathophysiology of vascular diseases including hypertension, atherosclerosis and myocardial infarction[1–3]. Vascular tone is regulated by the contraction of vascular smooth muscle cells (VSMC) in the blood vessel wall. VSM contraction is tightly coupled to the phosphorylation of the regulatory myosin light chain [4], which is regulated by the opposing activities of myosin light chain kinase (MLCK) and myosin light chain phosphatase (MLCP)(reviewed in[5]). MLCP dephosphorylates MLC leading to vascular smooth muscle relaxation (reviewed in[6, 7]). MLCP activity is highly

*Corresponding author: Molecular Cardiology Research Institute, Tufts Medical Center, Box 80, 800 Washington Street, Boston, MA 02111, Phone: 617-636-0619, Fax: 617-636-1444, E-mail: HSurks@tuftsmedicalcenter.org.

Disclosures: None.

regulated by both vasoconstrictor and vasodilator signaling pathways. Nitrovasodilators stimulate cGMP-dependent protein kinase 1α which activates MLCP to cause MLC dephosphorylation and smooth muscle relaxation[8–10]. Vasoconstrictors, conversely, inhibit MLCP leading to MLC phosphorylation and smooth muscle contraction (reviewed in [6]). Vasoconstrictor mediated MLCP inhibition occurs by either phosphorylation of the MLCP inhibitory protein CPI-17[11], or by phosphorylation of the myosin binding subunit (MBS) of MLCP at inhibitory sites T696 and T850[12–14].

The RhoA/ROCK pathway is the most extensively studied mechanism of MLCP inhibition. Vasoconstrictor G-protein coupled receptor agonists lead to activation of RhoA guanine nucleotide exchange factors and GTP loading of the monomeric GTPase RhoA[15]. GTP-bound RhoA then binds and activates its downstream effector ROCK[16–18] which in turn phosphorylates MBS[19] at the two phosphorylation sites [12, 13] leading to inhibition of MLCP activity[14]. Phosphorylation at T850 also has been shown to cause dissociation of MBS from myosin[20]. More recently, T850 has been implicated as the major ROCK phosphorylation site, whereas T696 is thought to be phosphorylated by other kinases[14]. Many studies support that RhoA/ROCK signaling plays a role in the regulation of vascular tone and in the pathogenesis of vascular diseases[21–25], yet the precise mechanisms by which ROCK is targeted to and interacts with MLCP are not well understood.

We and others have recently characterized a new member of the MLCP complex, myosin phosphatase-rho interacting protein (MP-RIP, also M-RIP, $p116^{RIP}$)[26–28]. MP-RIP is a cytoskeletal scaffold that binds directly to both RhoA and MBS[26] and targets MLCP to the contractile apparatus to dephosphorylate MLC[28, 29]. MP-RIP is also required to colocalize RhoA and MBS to regulate MLCP[30]. MP-RIP, however, does not bind ROCK[28], leaving the issue of how ROCK is targeted to MLCP unresolved.

There are two isoforms of ROCK, ROCK1 and 2, that share overall 65% homology at the amino acid level[31]. The tissue distribution of ROCK1 and 2 is similar, and relatively few studies have delineated the isoform specific roles of ROCK. Smooth muscle cells have been traditionally thought to express ROCK2 since it was purified from gizzard smooth muscle, although the expression of ROCK1 was not excluded [32]. In this study, the specific roles of the ROCK isoforms in MLCP regulation and VSMC contractility were explored.

Materials and Methods

Cell culture

A7r5 cells were purchased from ATCC. Primary rat aortic smooth muscle cells were derived from rat aortas by the explant method and were identified by the expression of smooth muscle alpha actin.

Smooth muscle cell contractility assay

Primary rat aortic smooth muscle cells were plated on a polymer substrate consisting of microfabricated posts made by replica molding of polydimethylsiloxane (PDMS). After incubation in serum-free media for 48 hrs the cells were stimulated with contractile agonist and imaged every minute for 30 minutes using a Cool SNAP EZ CCD camera (Photometrics) with NIS Elements software. Cell length change following agonist stimulation was measured using Image Pro Plus 6.0 software.

A detailed description of Materials and Methods can be found in the online data supplements.

Results

The MBS of MLCP interacts with ROCK2 in VSMCs

To investigate the mechanism whereby ROCK interacts with MLCP, ROCK1 and 2 were individually immunoprecipitated from A7r5 VSMCs without contamination by the other isoform (Figure 1A) [33]. When the ROCK1 and 2 immunopellets were probed for MBS binding, ROCK2, but not ROCK1, was found to co-immunoprecipitate MBS (Figure 1B). In primary rat aortic smooth muscle cells, where the immunoreactivity of ROCK1 and 2 was similar, MBS was also found selectively in the ROCK2 immunopellet (Figure 1C). In a separate approach, ROCK2, but not ROCK1 was found in a myc-MBS immunopellet from transfected HEK293 cells (Figure 1D). Together, these experiments support that the MBS of MLCP interacts specifically with ROCK2.

Cell stimulation augments the ROCK2-MBS interaction

The ROCK2-MBS co-immunoprecipitation in resting VSMCs was augmented by exposure to the contractile agonist LPA or to serum (Figure 2A). These stimuli would be expected to increase ROCK activity, and the data therefore suggest that ROCK activity may modulate its interaction with MBS. When the time course of ROCK2-MBS binding in response to serum was examined, the interaction was significantly increased within five minutes of stimulation ($p=0.008$, $n=4$), was diminished by forty minutes, and reached a second peak at one hour ($p=0.04$, $n=4$) (Figure 2B). When phosphorylation of MBS by ROCK was studied, a similar time course was observed ($p=0.04$ at 5 and 60 mins, $n=4$), suggesting that the ROCK2-MBS interaction correlates with phospho-regulation of MLCP by ROCK (Figure 2C).

Mechanism of ROCK-MBS binding

To localize the ROCK2 binding domains within MBS, GST-fusion proteins were created that together encompassed the entire MBS molecule. These were individually tested for binding to ROCK from VSMC lysates. MBS peptides corresponding to amino acids 540–858 (with and without the central insert splice variant) and 683–866 both bound ROCK2 (Figure 3A). The minimal MBS domain tested that bound ROCK included amino acids 683–866, which contain the two major inhibitory phosphorylation sites, T696 and T850 (Figure 3C) and a predicted coiled coil structure (amino acids 704 to 764). Interestingly, MBS 683–866 was able to bind both ROCK2 and ROCK1 *in vitro*. When binding of mycROCK1 and mycROCK2 to MBS 683–866 was compared, two fold more ROCK2 bound MBS than ROCK1 ($p=0.01$, $n=3$, Figure 3B). MP-RIP targets RhoA to regulate MLCP [26, 28, 30], however Koga and Ikebe recently found that MP-RIP does not interact with ROCK[28]. To confirm this observation in our binding studies, the same MBS domains were probed for MP-RIP binding. MP-RIP bound MBS 850–1030, confirming our previous findings [26] and demonstrating that MP-RIP and ROCK bind to distinct domains of MBS (Figure 3A). Furthermore, when GST-MP-RIP domains, together encompassing the entire molecule, were compared with GST-MBS 683–866 for ROCK binding, only GST-MBS bound ROCK (Online Figure 1).

To localize the MBS binding domain of ROCK, and to test direct binding between MBS and ROCK, four domains each of ROCK1 and 2, that together encompassed both molecules in their entirety, were separately tested for binding to GST-MBS 683–866. Of the ROCK2 domains, a coiled coil domain of ROCK2, 354–775, and to a much lesser extent the kinase domain of ROCK2, 1–360, bound MBS (Figure 3D). No domains of ROCK1 specifically bound MBS (Figure 3D and data not shown). The homology between ROCK2 354–775 and ROCK1 338–750 is only 58% (Online Figure 2), compared to 86% homology between the catalytic domains of the two isoforms (Data not shown). These studies suggest that ROCK2 amino acids 354–775 can directly bind MBS amino acids 683–866 (Figure 4).

ROCK isoform regulation of MLCP and MLC phosphorylation

When overexpressed in VSMCs, ROCK1 and 2 were localized diffusely in the cytoplasm (Figure 5A, right panels). Immunofluorescent labeling with phospho-MLC antibodies showed that overexpression of either ROCK1 or ROCK2 dramatically increased MLC phosphorylation (Figure 5A, left panels) whereas GFP did not affect MLC phosphorylation, and a dominant negative ROCK2 peptide reduced MLC phosphorylation in this assay (Online Figure 3).

When ROCK1 and 2 were individually silenced using RNAi, up-regulation of the other isoform was noted (Figure 5B). Combined ROCK isoform silencing was not as effective as individual silencing. MBS phosphorylation at the two inhibitory phosphorylation sites, T696 and T850, was probed in the setting of ROCK silencing. Silencing of either ROCK isoform caused a significant reduction in phosphorylation at T850 ($p<0.05$ for ROCK1 and ROCK2a, n=4) (Figure 5C). Silencing of both ROCK isoforms combined caused a significantly greater reduction in MBS T850 phosphorylation than individual silencing of either ROCK isoform ($p=0.04$ vs ROCK1 alone, n=4). ROCK silencing did not affect phosphorylation of MBS at T696 (Online Figure 4).

Phosphorylation of the MLCP downstream substrate MLC, the biochemical determinant of smooth muscle contraction, was also examined in the setting of ROCK isoform silencing. ROCK1 and 2 silencing both reduced MLC phosphorylation, although only ROCK2 silencing reached statistical significance ($p<0.002$, n=4) (Figure 5D). Combined ROCK silencing caused greater inhibition of MLC phosphorylation than silencing of individual ROCK isoforms ($p<0.05$ for R1,R2a or R2b vs R1+R2, n=4) (Figure 5D). When examined by immunofluorescence microscopy, silencing of either ROCK isoform reduced phosphorylation of MLC, consistent with the biochemical data above (Figure 5E). These studies support that the ROCK isoforms both regulate MLCP activity and MLC phosphorylation and have an additive effect when silenced in combination.

ROCK isoform regulation of VSMC morphology

The ROCK isoforms were found to have distinct morphologic effects on primary rat aortic smooth muscle cells (Figure 6A, Online Figures 5, 6). ROCK1 silenced cells had a smaller cell area (47% reduction, $p<0.001$ vs scrambled, one way ANOVA on ranks, Figure 6A, B), fewer stress fibers (39% reduction, $p<0.001$ vs scrambled, one way ANOVA on ranks, Figure 6A, C) and increased numbers of focal adhesions (40% increase, $p<0.05$, ANOVA Holm-Sidak test, Figure 6A, D) than scrambled control transfected cells. ROCK2 silenced cells had a larger cell area (65% increase, $p<0.001$ vs scrambled, one way ANOVA on ranks, Figure 6A, B) and greater number of stress fibers (49% increase, $p<0.001$ vs scrambled, one way ANOVA on ranks, Figure 6A, C) and fewer focal adhesions (63% reduction, $p<0.001$, ANOVA Holm-Sidak test, Figure 6A, D) compared to control VSMCs. These experiments support that whereas both ROCK isoforms regulate MBS and MLC phosphorylation, they have opposing effects on cell morphology. Treatment with the contractile agonist LPA modestly increased the number of stress fibers and reduced the number of focal adhesions under all silencing conditions (Online Figure 5). Treatment with the ROCK inhibitor Y27632 dramatically reduced the numbers of stress fibers and focal adhesions under all silencing conditions, indicating that ROCK activity was high even in the resting cells in which one ROCK isoform had been silenced (Online Figure 6).

ROCK isoform regulation of VSMC contractility

The role of the ROCK isoforms in VSMC contractility was explored using an assay in which VSMCs are cultured on microfabricated posts which do not hinder cell contraction and whose movement can be used to measure cellular force production [34–39]. Cells transfected with scrambled and ROCK2 siRNA were elongated, whereas cells transfected with ROCK1 siRNA

appeared smaller than scrambled control and ROCK2 silenced cells, consistent with the immunofluorescence labeling in Figure 6 (also Figure 7A and Online videos). When the contractile agonist LPA was applied, control cells underwent a gradual contraction, primarily along the long axis of the cells, over a period of 15–20 mins (see Online video 1). LPA-mediated contractions were abolished by pretreatment with the ROCK1 and ROCK2 inhibitor Y27632, supporting that the contractility was mediated by ROCK (Online Figure 7) and by pretreatment with blebbistatin, indicating that the contraction required actin-myosin interactions (Online Figure 8). ROCK1 silenced VSMCs also underwent a vigorous contraction (Figure 7A and Online video 2). ROCK2 silenced cells contracted significantly less than scrambled control and ROCK1 silenced cells (Figure 7A, B, and Online video 3. $P<0.001$ vs scrambled siRNA cells, one way ANOVA).

Intracellular force generation was calculated from the displacement of microfabricated posts. Force maps of control, ROCK1 and ROCK2 silenced cells (Figure 7A) confirmed that ROCK1 silencing did not significantly affect force generation, whereas ROCK2 silencing significantly reduced force (Figure 7C, Scrambled vs. ROCK1, p=NS, Scrambled vs. ROCK2, $p<0.05$, ANOVA on ranks). Interestingly, the difference in force between ROCK2 and controls cells was more pronounced than the difference in cell contraction in Figure 7B. When examined in more detail, control and ROCK1 silenced cells had a similar relationship between force production and the degree of contraction. However, ROCK2 silenced cells exhibited a steeper slope for this relationship, indicating that force production yielded a greater degree of contraction in these cells (Figure 7D).

The differences in force production and contraction between ROCK1 and ROCK2 silenced cells were explored further using immunofluorescence microscopy to image actin-myosin fibers and phosphorylation of MLC after treatment with LPA or Y27632 (Figure 7E, Online Figures 9, 10). The stress fibers in control silenced VSMCs were aligned with and extended across the long axis of the cell, and were diffusely localized throughout the cell body. The stress fibers displayed abundant MLC phosphorylation despite lack of agonist stimulation (Figure 7E). ROCK1 silenced cells had fewer stress fibers than control cells, yet these stress fibers extended across the long axis of the cell, and were frequently localized at the cell periphery. MLC phosphorylation colocalized with the peripheral actin-myosin stress fibers (Figure 7E). The ROCK2 silenced cells displayed abundant stress fibers, but in many cells the stress fibers were short and haphazardly arranged. MLC phosphorylation also colocalized with stress fibers in the ROCK2 silenced cells (Figure 7E). For all silencing conditions, stimulation with LPA increased both stress fiber number and MLC phosphorylation slightly (Online Figure 9), whereas Y27632 dramatically reduced both stress fiber number and MLC phosphorylation (Online Figure 10). The differences in stress fiber distribution and orientation between ROCK1 and ROCK2 silenced VSMCs raised the possibility that the axis of force generation may be altered when ROCK isoform expression is silenced. The direction of movement of the microfabricated posts was used to determine the average longitudinal and transverse components of force, which were plotted for each silencing condition (Figure 7F). For both scrambled and ROCK1 silenced cells, the longitudinal and transverse forces were similar and the force vectors pointed toward the center of the cell. However, in ROCK2 silenced cells, the force vectors were random and small, possibly reflecting the haphazard distribution of stress fibers as seen in Figures 5E, 6A and 7E.

Discussion

There is little known about the ROCK isoform specificity of MLCP regulation or the mechanism whereby ROCK interacts with MLCP. We have found that ROCK2 specifically is found in a complex with MBS in the cell. Although MP-RIP targets RhoA to MLCP[30], MP-RIP does not bind ROCK[28]. Our data confirm that ROCK and MP-RIP bind separate domains

of MBS. The data presented here support a model where RhoA bound to MP-RIP and ROCK bound to MBS are brought into proximity by MP-RIP/MBS binding.

In the first demonstration of ROCK2-MLCP binding, we found that amino acids 683–866 bind directly to amino acids 354–775 of ROCK2. The ROCK2 binding domain on MBS is predicted to contain a coiled coil structure between amino acids 704 and 764. The MBS binding domain of ROCK2, amino acids 354–775, is also predicted to be a coiled coil structure, suggesting that coiled-coil binding mediates their interaction. Future studies will further characterize the specific residues involved in their interaction. Although ROCK1 338–750 is also predicted to form a coiled coil, the amino acid homology between ROCK1 and 2 in this domain is only 58%, suggesting that the specific residues that mediate the ROCK2-MBS interaction differ between the two ROCK isoforms. In fact, this domain of ROCK1, but not ROCK2, has been found to bind to RhoE and PDK1, further supporting that this region of ROCK1 and ROCK2 mediates isoform-specific interactions [40, 41]. Interestingly, in GST-fusion protein interaction assays, both ROCK1 and 2 from cell lysates could interact with MBS 683–866. However, twice as much ROCK2 bound MBS. These data suggest that there may be an intermediary protein (s) involved in ROCK1-MBS binding and that this interaction may become apparent when relatively high concentrations of GST-MBS peptide are used for binding studies. This potential indirect interaction between ROCK1 and MBS will require further investigation.

When the roles of the ROCK isoforms in MBS and MLC phosphorylation were tested, overexpression of both isoforms increased MLC phosphorylation. A previous study has shown that the ROCK isoforms lose their specificity when overexpressed [33], and therefore silencing studies were also undertaken. Interestingly, silencing of each ROCK isoform lead to up-regulation of the other isoform, suggesting that the expression level of the ROCK isoforms is tightly controlled and inter-related in VSMCs. Silencing of either ROCK isoform lead to reduced MBS and MLC phosphorylation. Furthermore, combined ROCK isoform silencing, despite that down-regulation of the ROCK isoforms was less efficient, lead to a significantly greater reduction in MBS and MLC phosphorylation than either isoform alone. These data support that both ROCK isoforms regulate MBS and MLC phosphorylation in VSMCs, and further, taken together with the binding data showing different mechanisms of interaction with MBS, suggest that their respective mechanisms are potentially distinct.

ROCK is known to regulate cell morphology, including the formation of actin-myosin stress fibers and focal adhesion complexes. Recently, two studies examined the roles of ROCK1 and 2 on fibroblast morphology with different results[33 42], and thus the effects of the ROCK isoforms on actin cytoskeletal architecture remains unresolved. In VSMCs, ROCK1 and ROCK2 had opposing effects, suggesting a cooperative role for the two ROCK isoforms where both are required to regulate cell morphology.

The measurement of contractility in single VSMCs is complicated by the strong focal adhesion contacts between the VSMC and the underlying substrate, limiting the cell's movement. This limitation has been addressed previously by plating VSMCs on flexible polymer substrates that can be pulled by the contracting cell. Force can be estimated by counting wrinkles in the polymer substrate, or by measuring the movement of beads embedded in the polymer. In this study, a recently developed technology to precisely calculate intracellular forces from single cells was adapted to measure contractility in VSMCs in which ROCK1 or ROCK2 expression was silenced.

The current study is the first to demonstrate that ROCK2 is the isoform that regulates VSMC force production and contractility. Furthermore, the specificity of ROCK2 for direct MLCP binding suggests that this interaction may be critical for contractile regulation, and is thus a potential target for the treatment of cardiovascular diseases. The regulation of actin cytoskeletal

organization may also contribute to the differential roles of the ROCK isoforms in contractility. The plot of force direction versus contraction axis suggests that force remains aligned with the major axes of the cell in ROCK1 but not in ROCK2 silenced cells. This is corroborated by immunofluorescence microscopy showing preserved phospho-MLC along the long axis of the cell in ROCK1 silenced cells, but in fragmented multidirectional fibers in ROCK2 silenced cells. These data suggest that the abnormal distribution of actin-myosin fibers may cause a disorganized orientation of force production and thus contribute to the reduced contraction in ROCK2 silenced VSMCs. These data further suggest that both force production and the orientation of force producing fibers are important in VSMC contractility. Interestingly, the reduction in force production in ROCK2 silenced cells was more pronounced than the reduction in contractility. This discrepancy may be related to the fewer focal adhesions in ROCK2 silenced cells, causing reduced tethering of the cell to the microfabricated posts and allowing more length change per unit of force.

The role of the RhoA/ROCK signaling pathway in the regulation of vascular smooth muscle contractility and vascular tone is well established, though the mechanisms are incompletely understood. ROCK inhibitors have been shown to ameliorate vascular disease in animal models and are promising future therapies for human cardiovascular disease (reviewed in [43]). Although relatively specific for ROCK, the inhibitors may be active against other kinases, and do not exhibit specificity for the individual ROCK isoforms[44]. A careful dissection of the specific roles of the two ROCK isoforms in vascular function may provide the opportunity to create therapies that target specific ROCK-mediated functions, while leaving other essential ROCK functions intact. This study indicates that whereas a balance of ROCK1 and ROCK2 activities is required to regulate VSMC actin cytoskeletal structure, ROCK2 is the predominant isoform that regulates VSMC contractility.

Supplementary Material

Refer to Web version on PubMed Central for supplementary material.

Acknowledgements

The authors wish to thank Dr. Shuh Narumiya for the ROCK1 and 2 cDNA, Dr. Masumi Eto for the MYPT1 cDNA, and Dr. Kozo Kaibuchi for the ROCK-Rho-binding domain cDNA. The authors also wish to thank Drs. Richard Karas and Michael E. Mendelsohn for helpful discussions.

Sources of Funding: Supported by NIH grants HL074069 and HL077378 to HKS. Dr. Zhang has grant support from the National Science Foundation.

Reference List

1. Stemerman MB, Ross R. Experimental arteriosclerosis. Fibrous plaque formation in primates, an electron microscope study. J Exp Med 1972;136:769–89. [PubMed: 4626850]
2. Goldberg ID, Stemerman MB, Schnipper LE, Ransil BJ, Crooks GW, Fuhro RL. Vascular smooth muscle cell kinetics: a new assay for studying patterns of cellular proliferation in vivo. Science 1979;295:920–2. [PubMed: 472713]
3. Stary HC. Evolution and progression of atherosclerotic lesions in coronary arteries of children and young adults. Arteriocsclerosis 1989;(Suppl I):I-19–I-32.
4. Hartshorne, DJ. Biochemistry of the contractile process in smooth muscle. In: Johnson, DR., editor. Physiology of the Gastrointestinal Tract. Vol. 2. New York: Raven; 1987. p. 423-82.
5. Somlyo AP, Somlyo AV. Signal transduction and regulation in smooth muscle. Nature 1994;372:231–6. [PubMed: 7969467]
6. Somlyo AP, Somlyo AV. Calcium Sensitivity of Smooth Muscle and Nonmuscle Myosin II: Modulated by G Proteins, Kinases and Myosin Phosphatase. Physiol Rev 2003;83:1325–1358. [PubMed: 14506307]

7. Hartshorne DJ, Ito M, Erdodi F. Role of Protein Phosphatase 1 in Contractile Functions: Myosin Phosphatase. J Biol Chem 2004;279:37211–37214. [PubMed: 15136561]

8. Surks HK, Mochizuki N, Kasai Y, Georgescu SP, Tang KM, Ito M, Lincoln TM, Mendelsohn ME. Regulation of Myosin Phosphatase by a Specific Interaction with cGMP-dependent Protein Kinase 1 alpha. Science 1999;286:1583–7. [PubMed: 10567269]

9. Wu X, Somlyo AV, Somlyo AP. Cyclic GMP-Dependent Stimulation Reverses G-Protein-Coupled Inhibition of Smooth Muscle Myosin Light Chain Phosphatase. Biochem Biophys Res Com 1996;220:658–63. [PubMed: 8607821]

10. Lee MR, Li L, Kitazawa T. Cyclic GMP Causes Ca+2 Desensitization in Vascular Smooth Muscle by Activating the Myosin Light Chain Phosphatase. J Biol Chem 1997;272:5063–8. [PubMed: 9030570]

11. Eto M, Kitazawa T, Yazawa M, Mukai H, Ono Y, Brautigan DL. Histamine-induced Vasoconstriction Involves Phosphorylation of a Specific Inhibitor Protein for Myosin Phosphatase by Protein Kinase C Isoforms. J Biol Chem 2001;276:29072–8. [PubMed: 11397799]

12. Feng J, Ito M, Ichikawa K, Isaka N, Nishikawa M, Hartshorne DJ, Nakano T. Inhibitory Phosphorylation Site for Rho-associated Kinase on Smooth Muscle Myosin Phosphatase. J Biol Chem 1999;274:37385–90. [PubMed: 10601309]

13. Kawano Y, Fukata Y, Oshiro N, Amano M, Nakamura T, Ito M, Matsumura F, Inagaki M, Kaibuchi K. Phosphorylation of Myosin-binding Subunit (MBS) of Myosin Phosphatase by Rho-Kinase In Vivo. J Cell Biol 1999;147:1023–37. [PubMed: 10579722]

14. Muranyi A, Derkach D, Erdodi F, Kiss A, Ito M, Hartshorne DJ. Phosphorylation of Thr696 and Thr850 on the myosin phosphatase target subunit: Inhibitory effects and occurrence in A7r5 cells. FEBS Let 2005;579:6611–6615. [PubMed: 16297917]

15. Noda M, Yasuda-Fukazawa C, Moriishi K, Kato T, Okuda T, Kurokawa K, Takuwa Y. Involvement of rho in GTPgammaS-induced enhancement of phosphorylation of 20kDa myosin light chain in vascular smooth muscle cells: inhibition of phosphatase activity. FEBS Let 1995;367:246–50. [PubMed: 7607316]

16. Matsui T, Amano M, Yamamoto T, Chihara K, Nakafuku M, Ito M, Nakano T, Okawa K, Iwamatsu A, Kaibuchi K. Rho-associated kinase, a novel serine/threonine kinase, as a putative target for the small GTP binding protein Rho. EMBO Journal 1996;15:2208–16. [PubMed: 8641286]

17. Ishizaki T, Naito M, Fujisawa K, Maekawa M, Watanabe N, Saito Y, Narumiya S. p160ROCK, a Rho-associated coiled-coil forming protein kinase, works downstream of Rho and induces focal adhesions. FEBS Let 1997;404:118–124. [PubMed: 9119047]

18. Leung T, Manser E, Tan L, Lim L. A Novel Serine/Threonine Kinase Binding the Ras-related RhoA GTPase Which Translocates the Kinase to Peripheral Membranes. J Biol Chem 1995;270:29051–4. [PubMed: 7493923]

19. Kimura K, Ito M, Amano M, Chihara K, Fukata Y, Nakafuku M, Yamamori B, Feng J, Nakano T, Okawa K, Iwamatsu A, Kaibuchi K. Regulation of Myosin Phosphatase by Rho and Rho-Associated Kinase (Rho-Kinase). Science 1996;273:245–8. [PubMed: 8662509]

20. Velasco G, Armstrong C, Morrice N, Frame S, Cohen P. Phosphorylation of the regulatory subunit of smooth muscle protein phosphatase 1M at Thr850 induces its dissociation from myosin. FEBS Let 2002;101:527.

21. Sawada N, Itoh H, Ueyama K, Yamashita J, Doi K, Chun T-H, Inoue M, Masatsugu K, Takatoshi S, Fukunaga Y, Sakaguchi S, Arai H, Ohno N, Komeda M, Nakao K. Inhibition of Rho-associated Kinase Results in Suppression of Neointimal Formation of Balloon-Injured Arteries. Circulation 2000;101:2030–3. [PubMed: 10790342]

22. Uehata M, Ishizaki T, Satoh H, Ono T, Kawahara T, Morishita T, Tamakawa H, Yamagami K, Inui J, Maekawa M, Narumiya S. Calcium sensitization of smooth muscle mediated by a Rho-associated protein kinase. Nature 1997;389:990–4. [PubMed: 9353125]

23. Shibata R, Kai H, Seki Y, Kato S, Morimatsu M, Kaibuchi K, Imaizumi T. Role of Rho-associated kinase in neointima formation after vascular injury. Circulation 2001;103:284–9. [PubMed: 11208690]

24. Matsumoto Y, Uwatoku T, Oi K, Abe K, Hattori T, Morishige K, Eto Y, Fukumoto Y, Nakamura K, Shibata Y, Matsuda T, Takeshita A, Shimokawa H. Long-Term Inhibition of Rho-Kinase Suppresses

Neointimal Formation After Stent Implantation in Porcine Coronary Arteries. Arterioscler Thromb Vasc Biol 2004;24:181–186. [PubMed: 14592842]

25. Miyata K, Shimokawa H, Kandabashi T, Higo T, Morishige K, Eto Y, Egashira K, Kaibuchi K, Takeshita A. Rho-Kinase is Involved in Macrophage-Mediated Formation of Coronary Vascular Lesions in Pigs In Vivo. Arterioscler Thromb Vasc Biol 2000;20:2351–2358. [PubMed: 11073837]
26. Surks HK, Richards CT, Mendelsohn ME. Myosin Phosphatase-Rho Interacting Protein: A New Member of the Myosin Phosphatase Complex that Directly Binds RhoA. J Biol Chem 2003;278:51484–93. [PubMed: 14506264]
27. Mulder J, Ariaens A, van den Boomen D, Moolenaar WH. p116RIP Targets Myosin Phosphatase to the Actin Cytoskeleton and Is Essential for RhoA/ROCK-regulated Neuritogenesis. Mol Biol of the Cell 2004;15:5516–27.
28. Koga Y, Ikebe M. p116RIP Decreases Myosin II Phosphorylation by Activating Myosin Light Chain Phosphatase and by Inactivating RhoA. J Biol Chem 2005;280:4983–91. [PubMed: 15545284]
29. Surks HK, Riddick N, Ohtani K. M-RIP Targets Myosin Phosphatase to Stress Fibers to Regulate Myosin Light Chain Phosphorylation in Vascular Smooth Muscle Cells. 280. J Biol Chem 2005;280:42543–42551. [PubMed: 16257966]
30. Riddick N, Ohtani K, Surks HK. Targeting by Myosin Phosphatase-RhoA Interacting Protein Mediates RhoA/ROCK Regulation of Myosin Phosphatase. J Cell Biochem 2007;103:1158–1170. [PubMed: 17661354]
31. Nakagawa O, Fujisawa K, Ishizaki T, Saito Y, Nakao K, Narumiya S. ROCK-I and ROCK-II, two isoforms of Rho-associated coiled-coil forming protein serine/threonine kinase in mice. FEBS Let 1996;392:189–193. [PubMed: 8772201]
32. Feng J, Ito M, Kureishi Y, Ichikawa K, Amano M, Isaka N, Okawa K, Iwamatsu A, Kaibuchi K, Hartshorne DJ, Nakano T. Rho-associated Kinase of Chicken Gizzard Smooth Muscle. J Biol Chem 1999;274:3744–52. [PubMed: 9920927]
33. Yoneda A, Multhaupt HA, Couchman JR. The Rho kinases I and II regulate different aspects of myosin II activity. J Cell Biol 2005;170:443–453. [PubMed: 16043513]
34. du Roure O, Saez A, Buguin A, Austin RH, Chavrier P, Siberzan P, Ladoux B. Force mapping in epithelial cell migration. Proc Natl Acad Sci 2005;102:2390–5. [PubMed: 15695588]
35. Saez A, Ghibaudo M, Buguin A, Silberzan P, Ladoux B. Rigidity-driven growth and migration of epithelial cells on microstructured anisotropic substrates. Proc Natl Acad Sci 2007;104:8281–6. [PubMed: 17488828]
36. Zhao Y, Lim CC, Sawyer DB, Liao R, Zhang X. Cellular force measurements using single-spaced polymeric microstructures: isolating cells from base substrate. J Micromech Microeng 2005;15:1649–56.
37. Zhao Y, Lim CC, Sawyer DB, Liao R, Zhang X. Simultaneous Orientation and Cellular Force Measurements in Adult Cardiac Myocytes Using Three-Dimensional Polymeric Microstructures. Cell Motil Cytoskel 2007;64:718–25.
38. Tan JL, Tien J, Pirone DM, Gray DS, Bhadriraju K, Chen CS. Cells lying on a bed of microneedles: An approach to isolate mechanical force. Proc Natl Acad Sci 2003;100:1484–9. [PubMed: 12552122]
39. Bhadriraju K, Yang M, Ruiz SA, Pirone D, Tan J, Chen CS. Activation of ROCK by RhoA is regulated by cell adhesion, shape and cytoskeletal tension. Exp Cell Res 2007;313:3616–23. [PubMed: 17673200]
40. Pinner S, Sahai E. PDK1 regulates cancer cell motility by antagonising inhibition of ROCK1 by RhoE. Nat Cell Biol 2008;10:127–37. [PubMed: 18204440]
41. Riento K, Guasch RM, Garg R, Jin B, Ridley AJ. RhoE Binds to ROCK1 and Inhibits Downstream Signaling. Mol Cell Biol 2003;23:4219–29. [PubMed: 12773565]
42. Darenfed H, Dayanandan B, Zhang T, Hsieh SH-K, Fournier AE, Mandato CA. Molecular Characterization of the Effects of Y-27632. Cell Motil Cytoskel 2007;64:97–109.
43. Budzyn K, Marley PD, Sobey CG. Targeting Rho and Rho-kinase in the treatment of cardiovascular disease. Trends in Pharmacological Sciences 2006;27:97–104. [PubMed: 16376997]
44. Narumiya, S.; Ishizaki, T.; Uehata, M. Use and Properties of ROCK-Specific Inhibitor Y-27632. In: Abelson, JN.; Simon, MI., editors. Methods in Enzymology. Academic Press; 2000. p. 273-84.

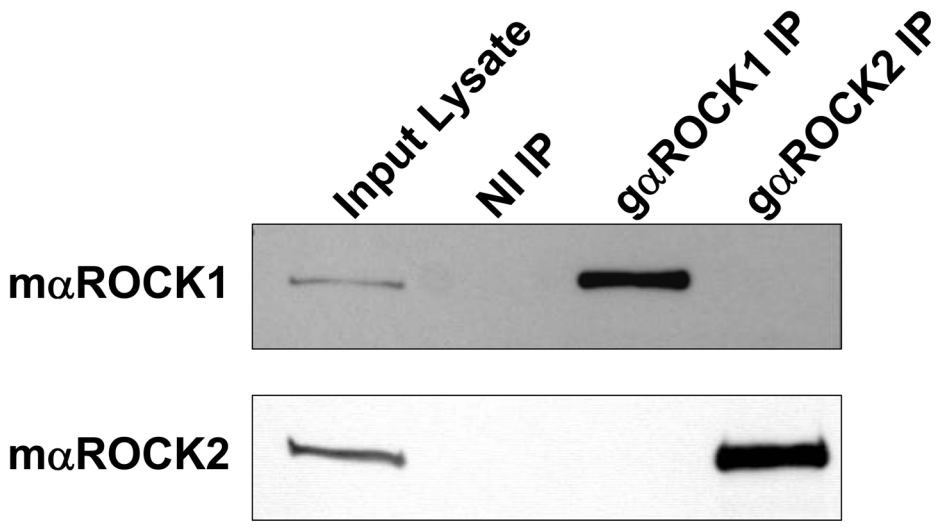

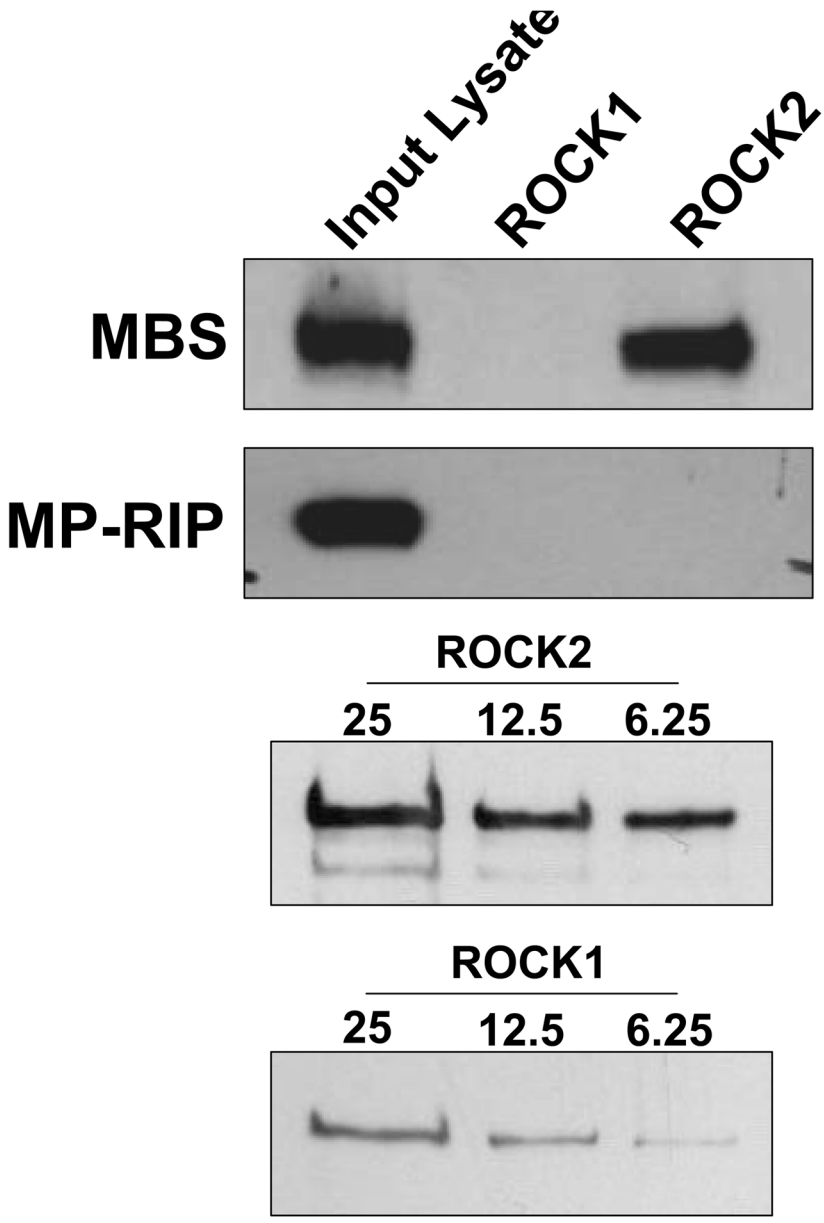

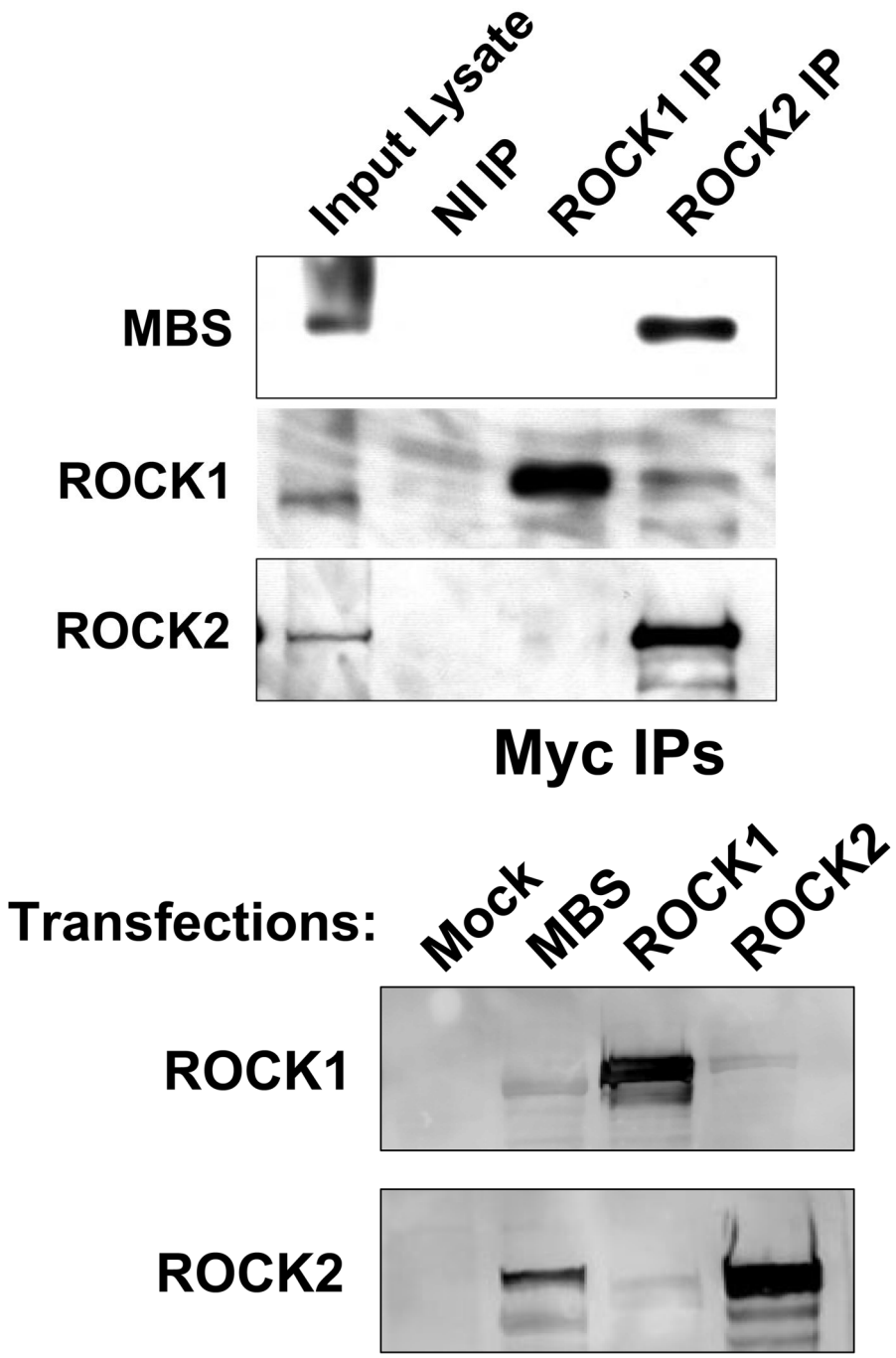

Figure 1. The MBS of MLCP interacts with ROCK2 in VSMCs

(A) ROCK1 and ROCK2 were immunoprecipitated from A7r5 cells using 1.4μg of either goat anti-ROCK1 (gαROCK1), goat anti-ROCK2 (gαROCK2) or goat non-immune (NI IP) antibodies. Immunoblots were performed with mouse anti-ROCK1 (mαROCK1) or mouse anti-ROCK2 (mαROCK2) antibodies. These conditions were used for all subsequent immunoprecipitations of ROCK1 and 2. (B) ROCK 1 and 2 were immunoprecipitated from A7r5 cells, followed by immunoblot to detect the MBS and MP-RIP proteins. A sample of the input protein for ROCK 1 and 2, 25, 12.5 and 6.25μg, is shown by immunoblot below. (C) Non-immune, ROCK1 and ROCK2 immunoprecipitations were performed from primary rat

aortic smooth muscle cells. The immunopellets were probed by immunoblot with MBS, ROCK1 and ROCK2 antibodies. (D) HEK293 cells were transfected with empty plasmid (Mock), and Myc-tagged MBS, ROCK1 or ROCK2. Immunoprecipitations were performed with anti-Myc antibodies, followed by immunoblotting for ROCK1 and ROCK2.

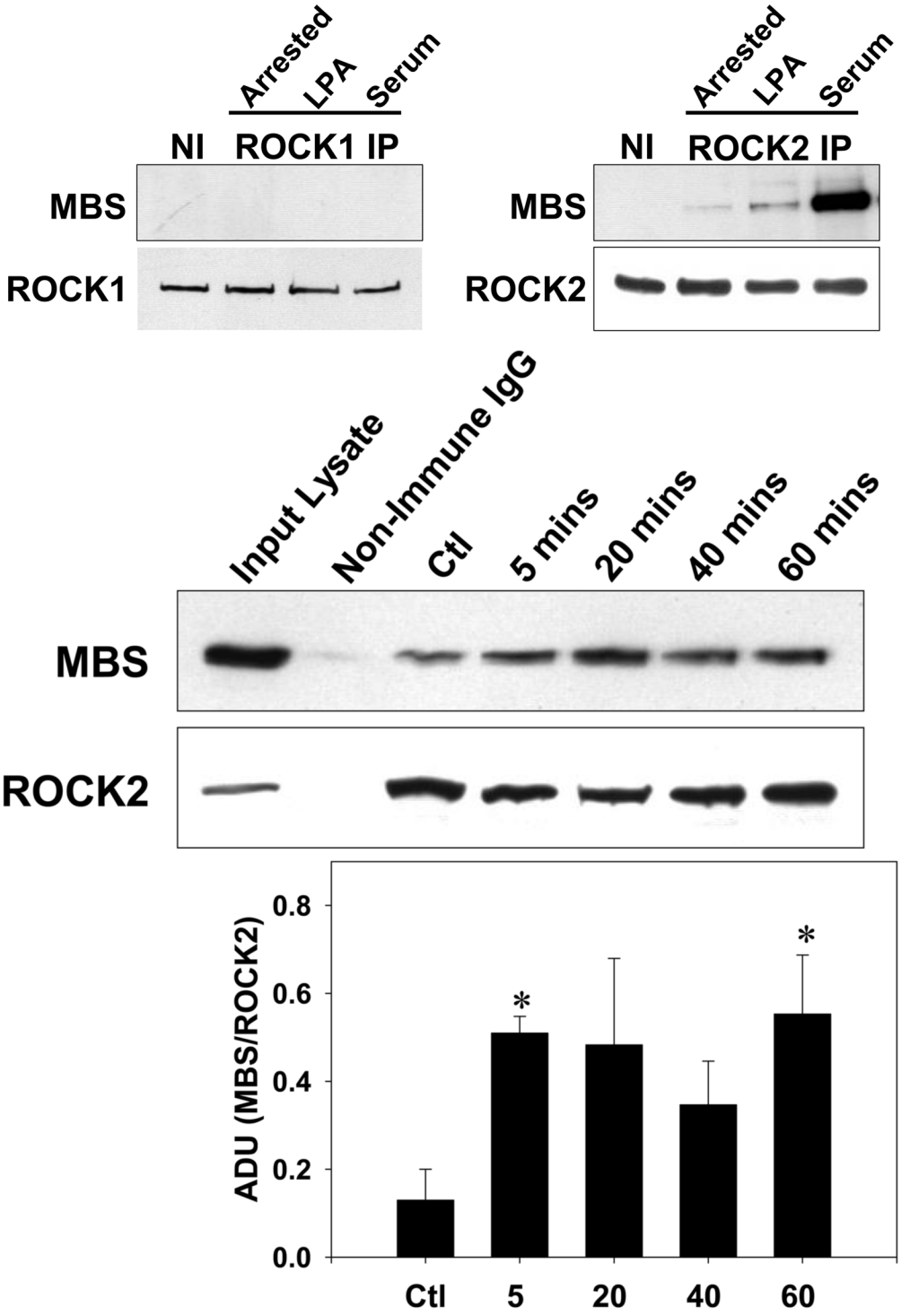

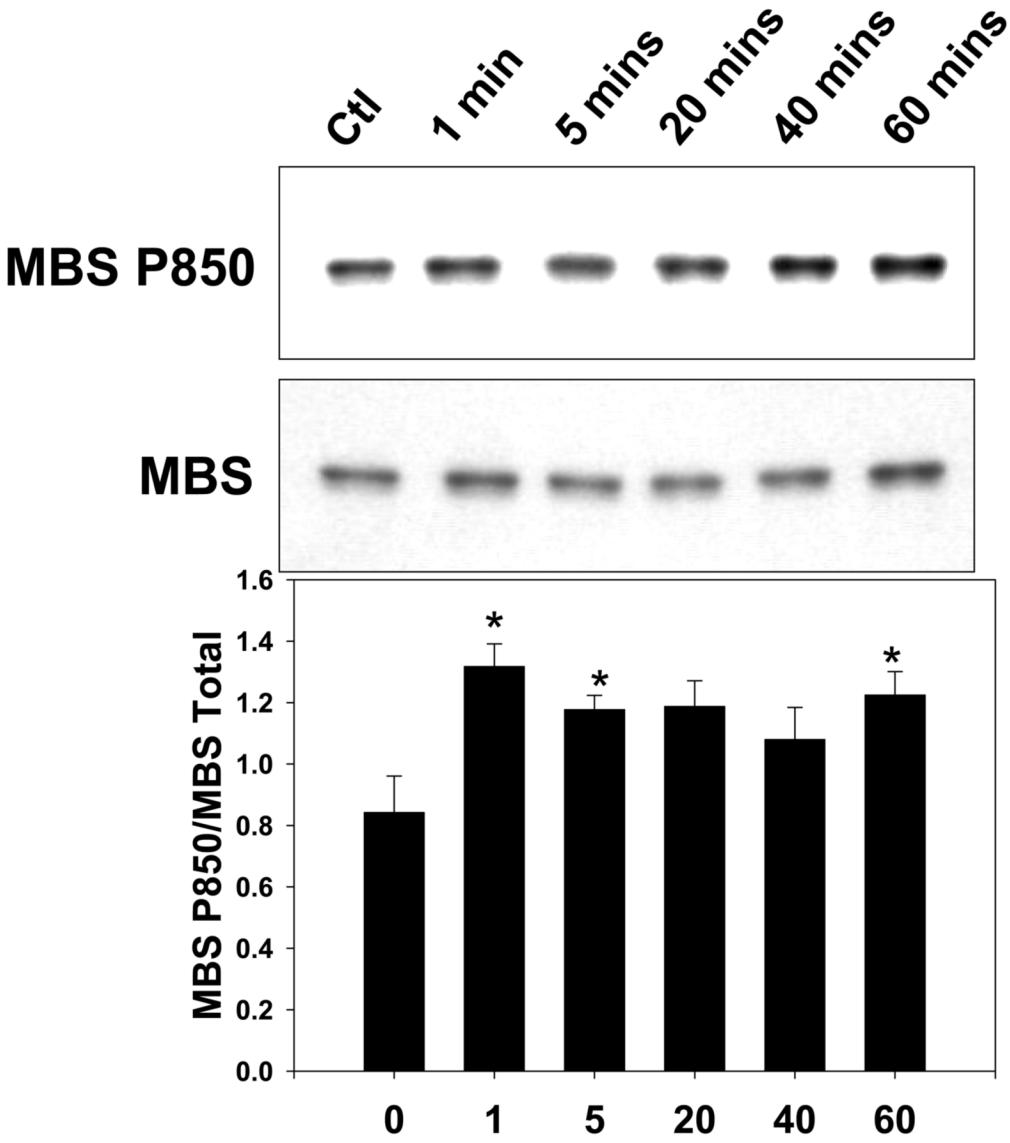

Figure 2. Cell stimulation augments the ROCK2-MBS interaction

(A) ROCK1 and 2 were immunoprecipitated from A7r5 cells in serum-free (arrested) conditions or following cell stimulation with either 1μM LPA or 10% serum. (B) A time-course of serum stimulation of A7r5 cells followed by ROCK2 immunoprecipitation is shown (Top). Pooled results from four experiments are shown on the bottom. (C) A time-course of serum stimulation of A7r5 cells followed by measurement of MBS phosphorylation at Thr850 by immunoblot (Top). Pooled results from four experiments (Bottom).

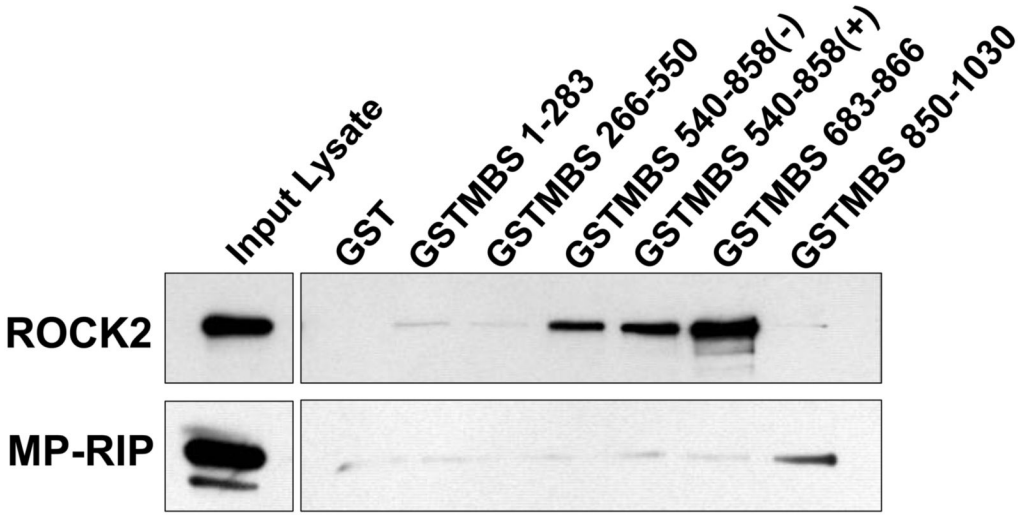

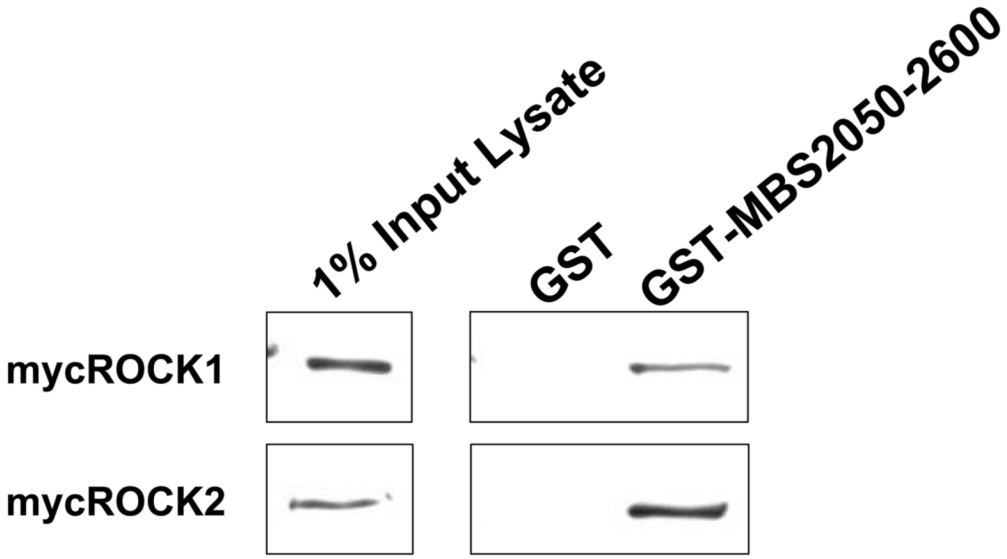

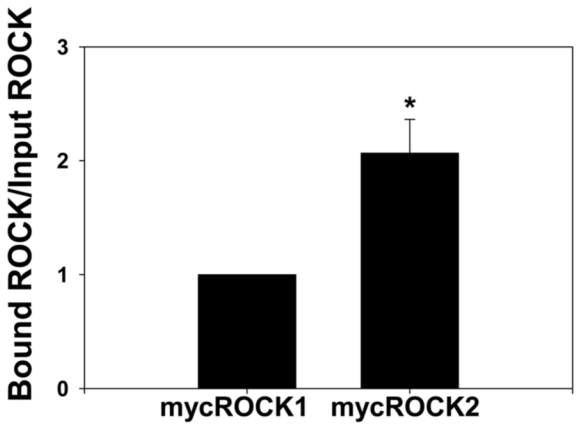

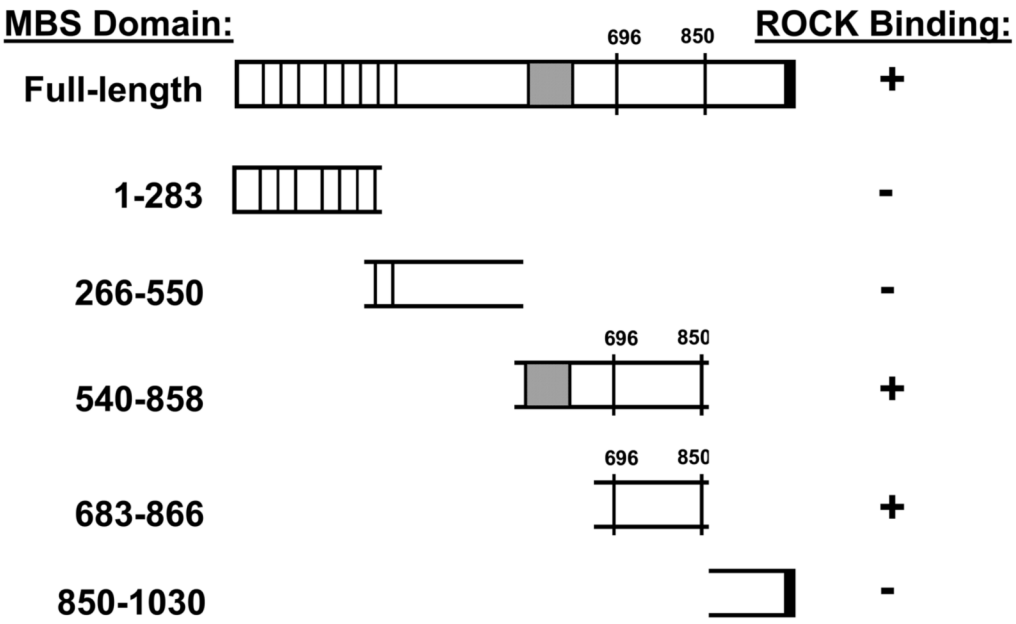

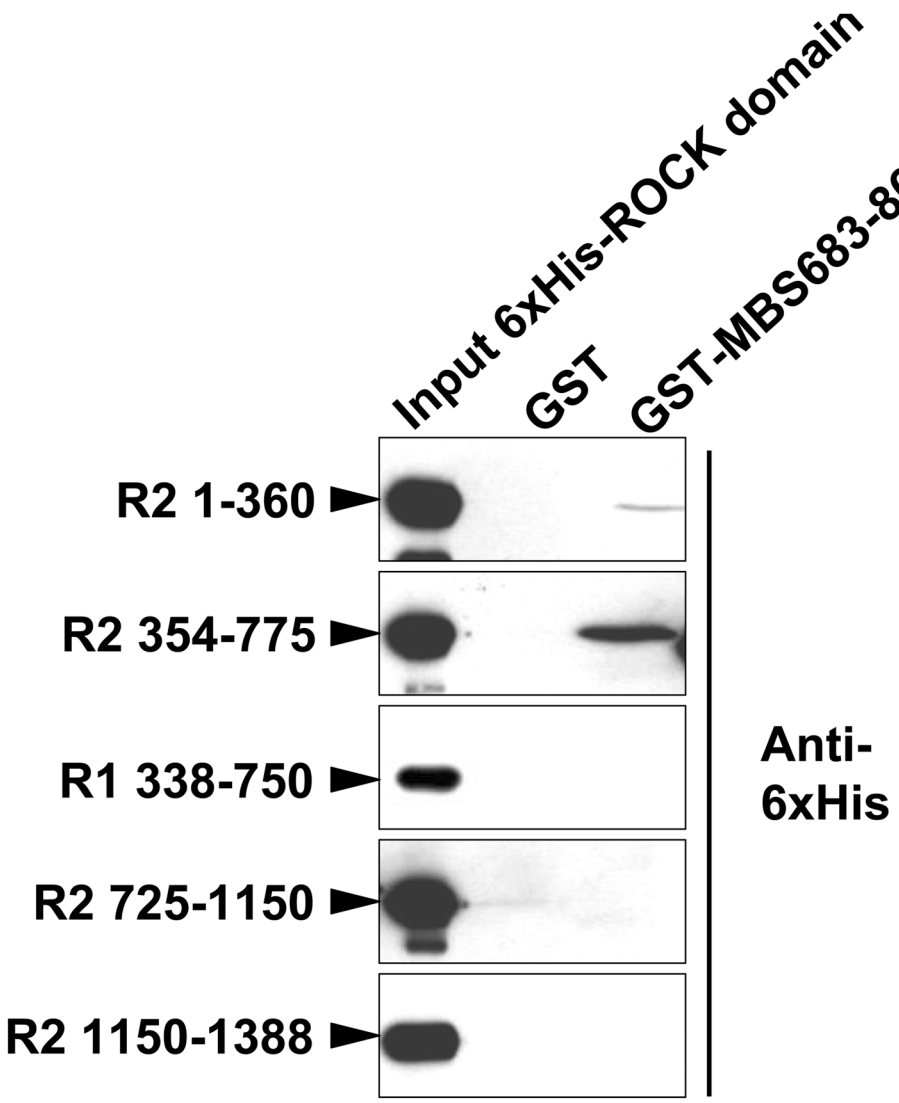

Figure 3. Mechanism of ROCK-MBS binding

(A) GST, and GST-fusion proteins (amino acid numbers noted, − and + indicate absence and presence of central insert splice variant) were tested for binding to ROCK2 and MP-RIP from A7r5 cell lysates. The input lysate is shown on the left for each protein. (B) GST and GST-MBS683–866 binding to mycROCK1 and mycROCK2 expressed in HEK293 cells. Input mycROCK1 and ROCK2 is shown on the left. Mean data from three experiments is shown. (C) Schematic diagram depicting the full-length MBS molecule, and each of the MBS peptides tested for ROCK binding. The amino acid residues are shown on the left, ROCK binding is shown on the right. The vertical lines in the MBS molecule represent the ankyrin repeats, the shaded box represents the central insert and 696 and 850 are the inhibitory phosphorylation sites. (D) Purified 6xHis-tagged ROCK2 (R2, numbers refer to amino acid residues) and ROCK1 (R1) domains were tested for binding to purified GST or GST-MBS683–866 using anti-6xHis antibodies.

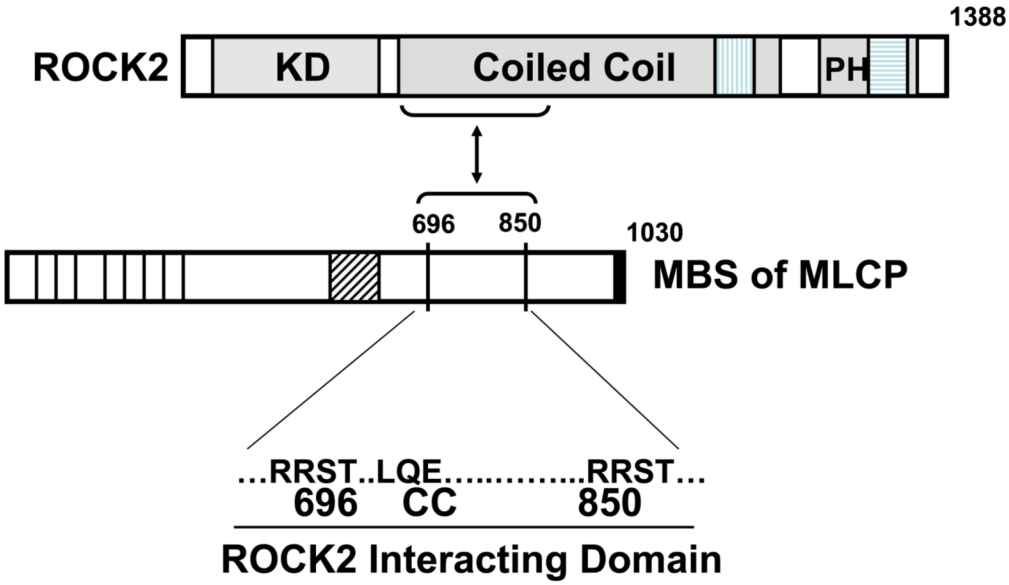

Figure 4. Direct binding interaction between ROCK2 and MBS

KD= kinase domain, PH=pleckstrin homology domain, vertical hatched box=RhoA binding domain, horizontal hatched box=cysteine rich domain. On MBS, vertical lines indicate ankyrin repeats, diagonal hatched box=central insert, 696 and 850 refer to the inhibitory phosphorylation sites, solid box is the leucine zipper domain. The blow-up region depicts the ROCK2 interacting domain, including both inhibitory phosphorylation sites, and a predicted coiled coil region.

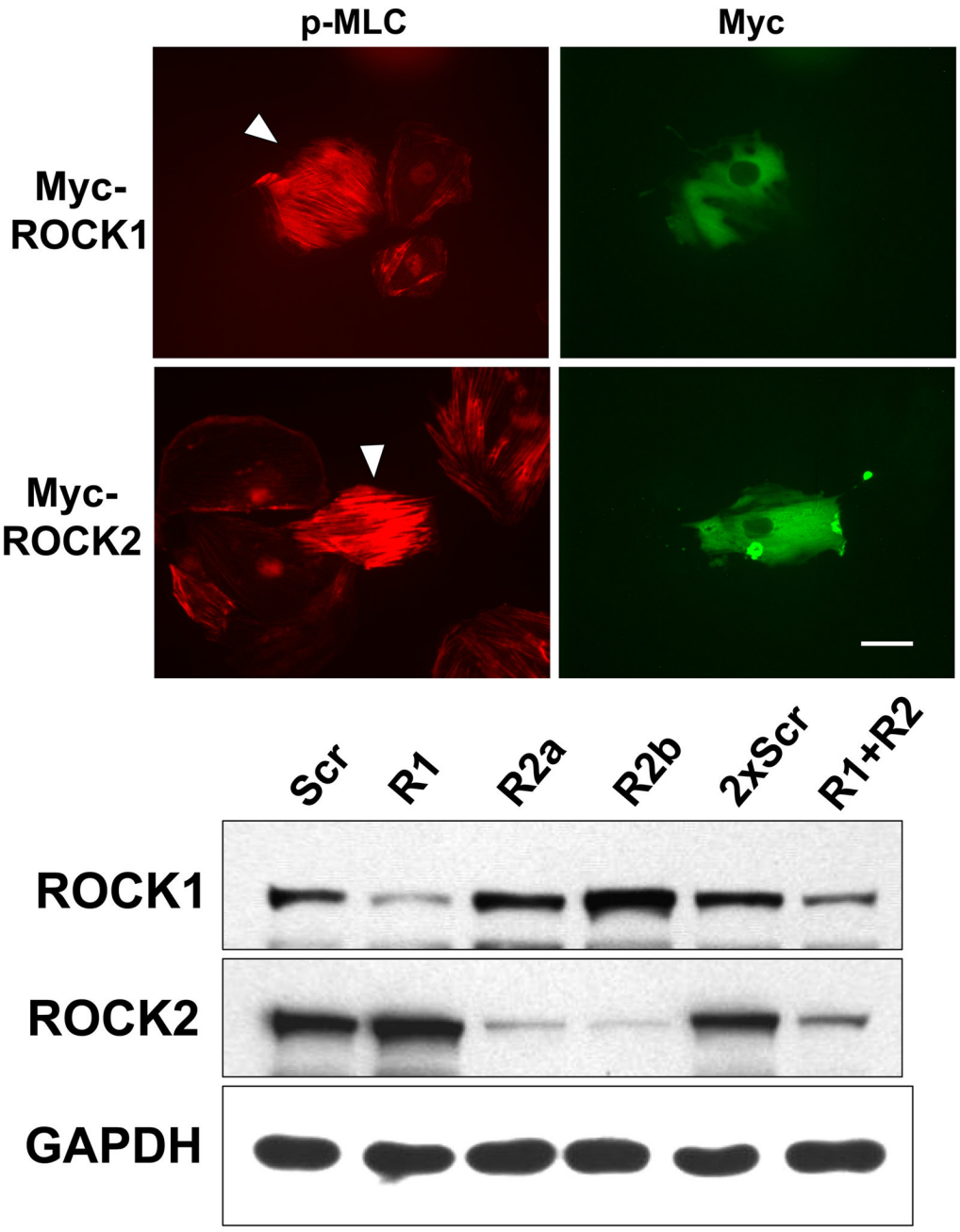

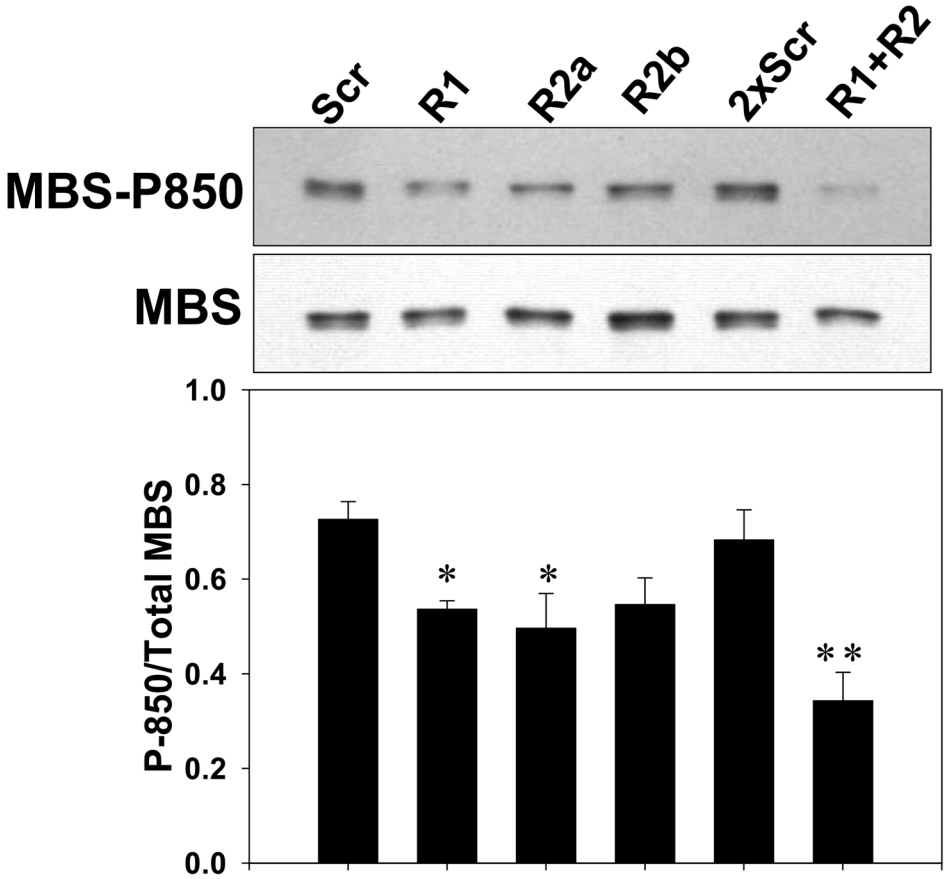

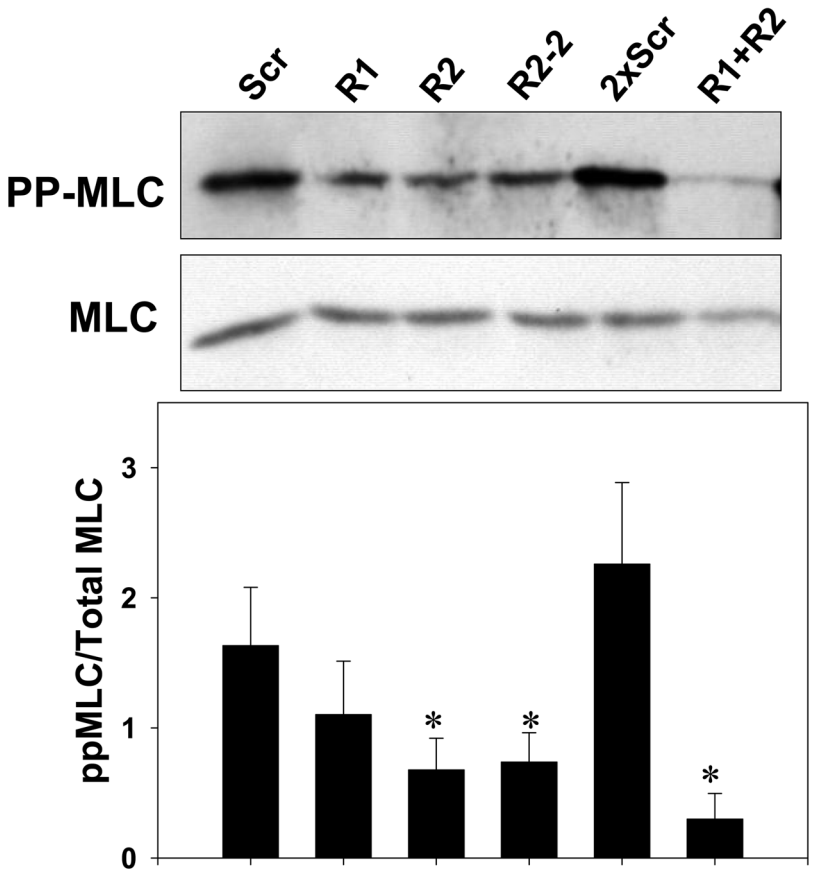

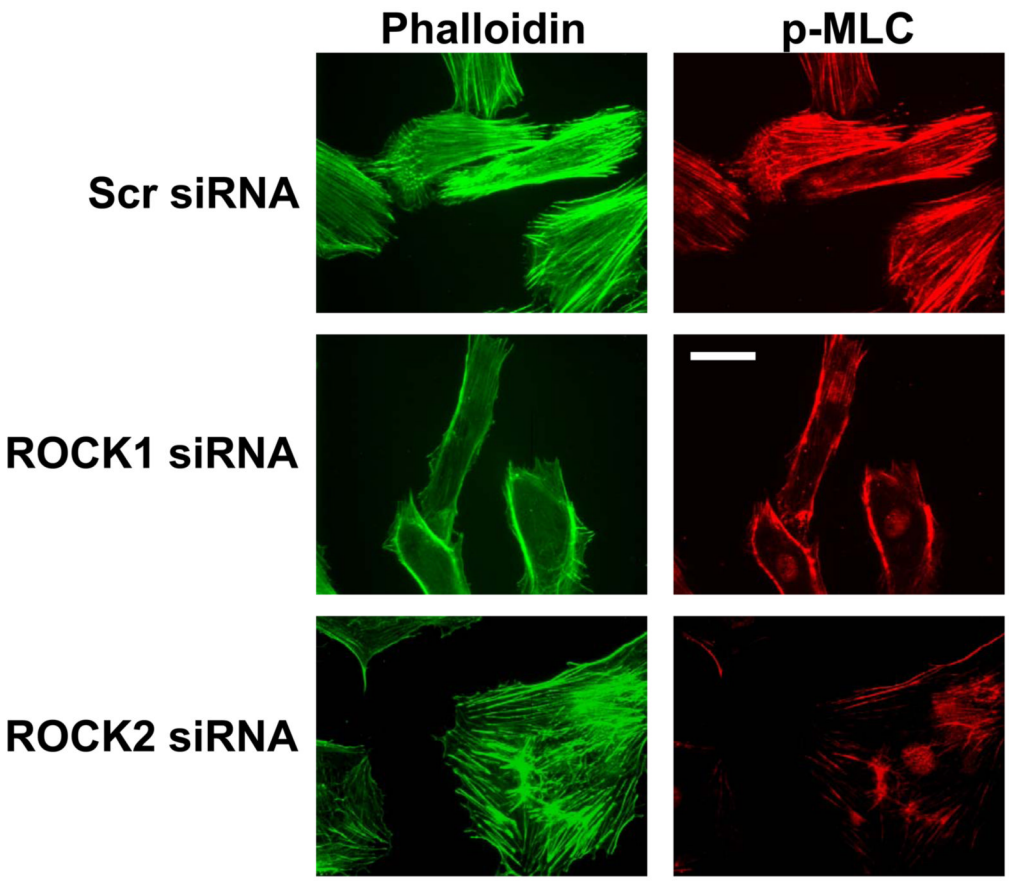

Figure 5. ROCK isoform regulation of MLCP and MLC phosphorylation

(A) A7r5 cells transfected with Myc-ROCK1 or Myc-ROCK2 and immunostained with both anti-phospho-MLC-Cy3 (left panels) and anti-Myc-FITC (right panels). The arrowheads indicated transfected cells. The scale bar is 30μm. (B) Immunoblot showing specific silencing of ROCK1 (R1) expression, ROCK2 (R2a and R2b, two separate oligonucleotides) expression or both ROCK1 and ROCK2 (R1+R2) expression in A7r5 cells using dsRNA oligonucleotides. Scr indicates scrambled negative control dsRNA (100nM). 2xScr indicates scrambled control dsRNA concentration adjusted to match R1+R2 (200nM). GAPDH is shown as a loading control. (C) Phosphorylation of MBS at the known inhibitory site Thr850 in A7r5 cells, following the silencing conditions described in 5B (Top). Total MBS is shown as a loading control. Pooled data from 4 experiments of MBS phosphorylation at Thr850 following ROCK isoform silencing (Bottom). The values are represented as Thr850 phosphorylation normalized to MBS expression for each sample. (D) Phosphorylation of MLC following silencing of ROCK isoforms in A7r5 cells as described in 5B (Top). Total MLC is shown as a loading control. Pooled data from 4 separate experiments of MLC phosphorylation following ROCK isoform silencing (Bottom). The values are represented as MLC phosphorylation normalized to total MLC expression for each sample. (E) Immunofluorescence microscopy of primary rat aortic smooth muscle cells following control (Scr) or ROCK isoform silencing. The cells were labeled with phalloidin to identify actin fibers (left column) and phospho-MLC (same antibody used for immunoblotting above) (right column). The scale bar is 30μm.

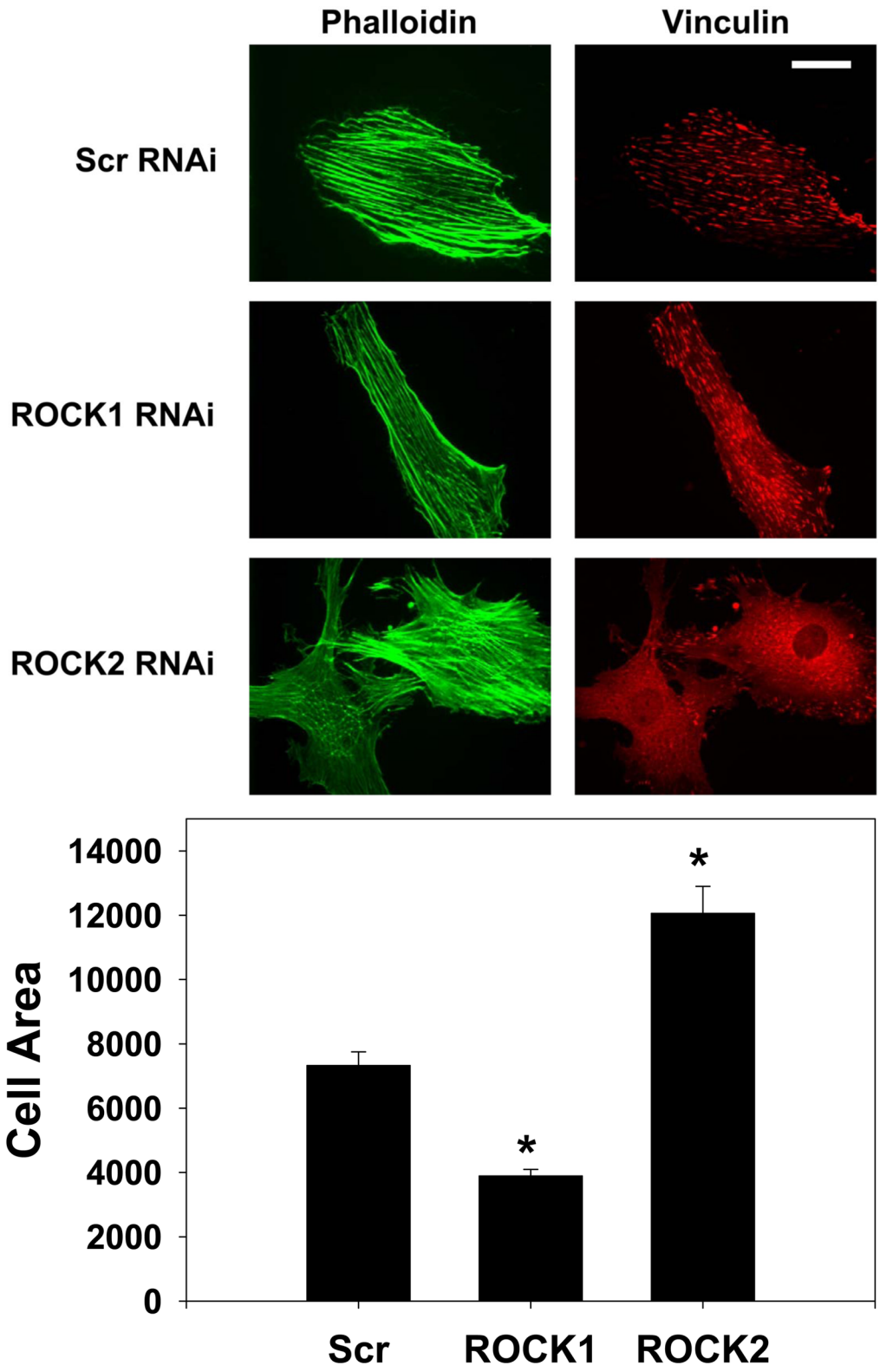

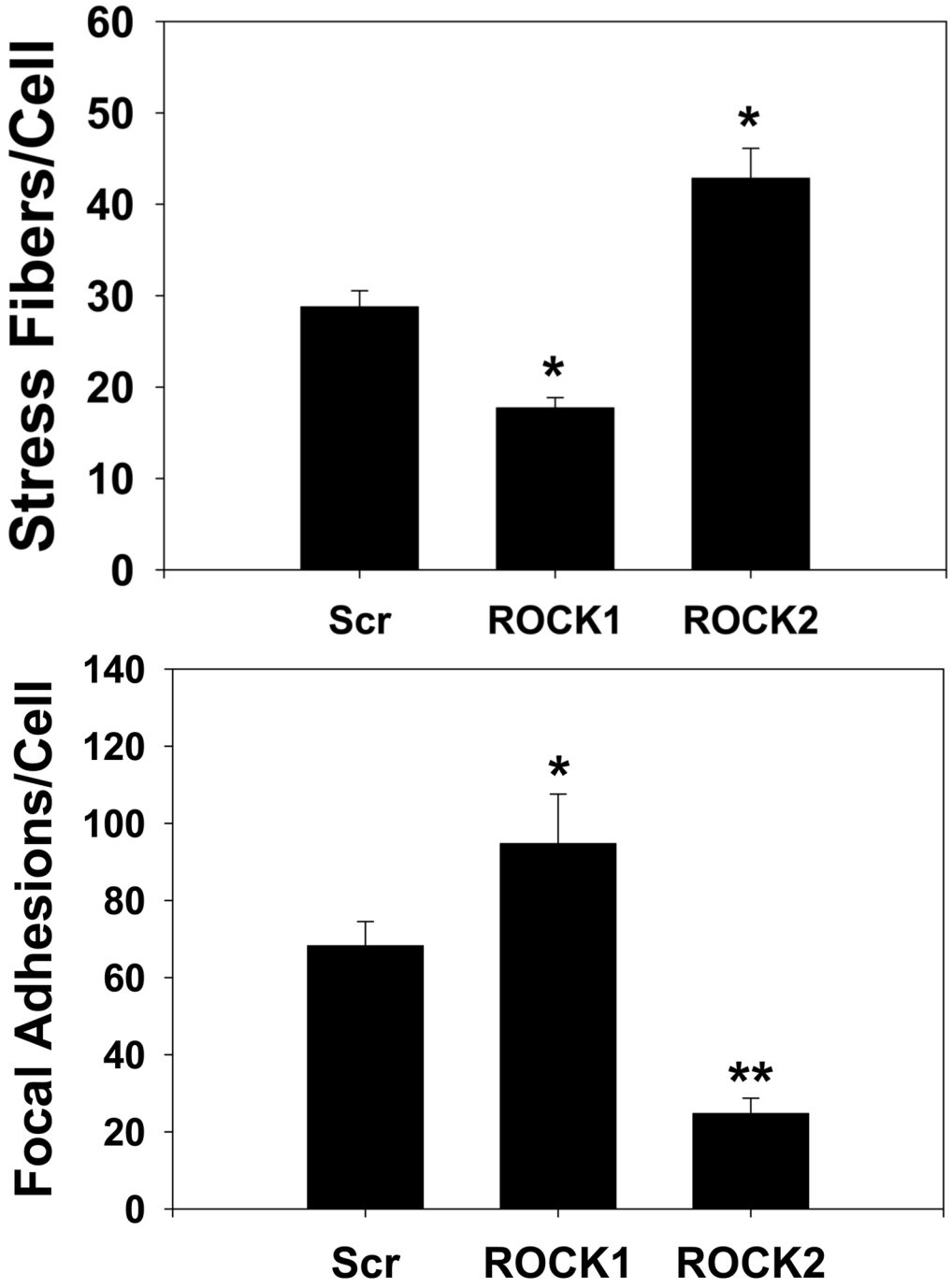

Figure 6. Morphology of ROCK1 and ROCK2 silenced VSMCs

(A) Immunofluorescence microscopy of representative primary rat aortic VSMCs plated on fibronectin coated coverslips and serum-deprived for 48 hours following scrambled negative control (Scr, top row), ROCK1 (middle row) and ROCK2 (bottom row) silencing and immunofluorescence labeling with phalloidin (left column) to image actin fibers and vinculin (right column) to image focal adhesions. (B) Cell area measurements of scrambled negative control (Scr), ROCK1 and ROCK2 silenced unstimulated VSMCs. (C) Stress fiber number in scrambled negative control (Scr), ROCK1 and ROCK2 silenced unstimulated VSMCs. (D)

Focal adhesion number in scrambled negative control (Scr), ROCK1 and ROCK2 silenced unstimulated VSMCs.

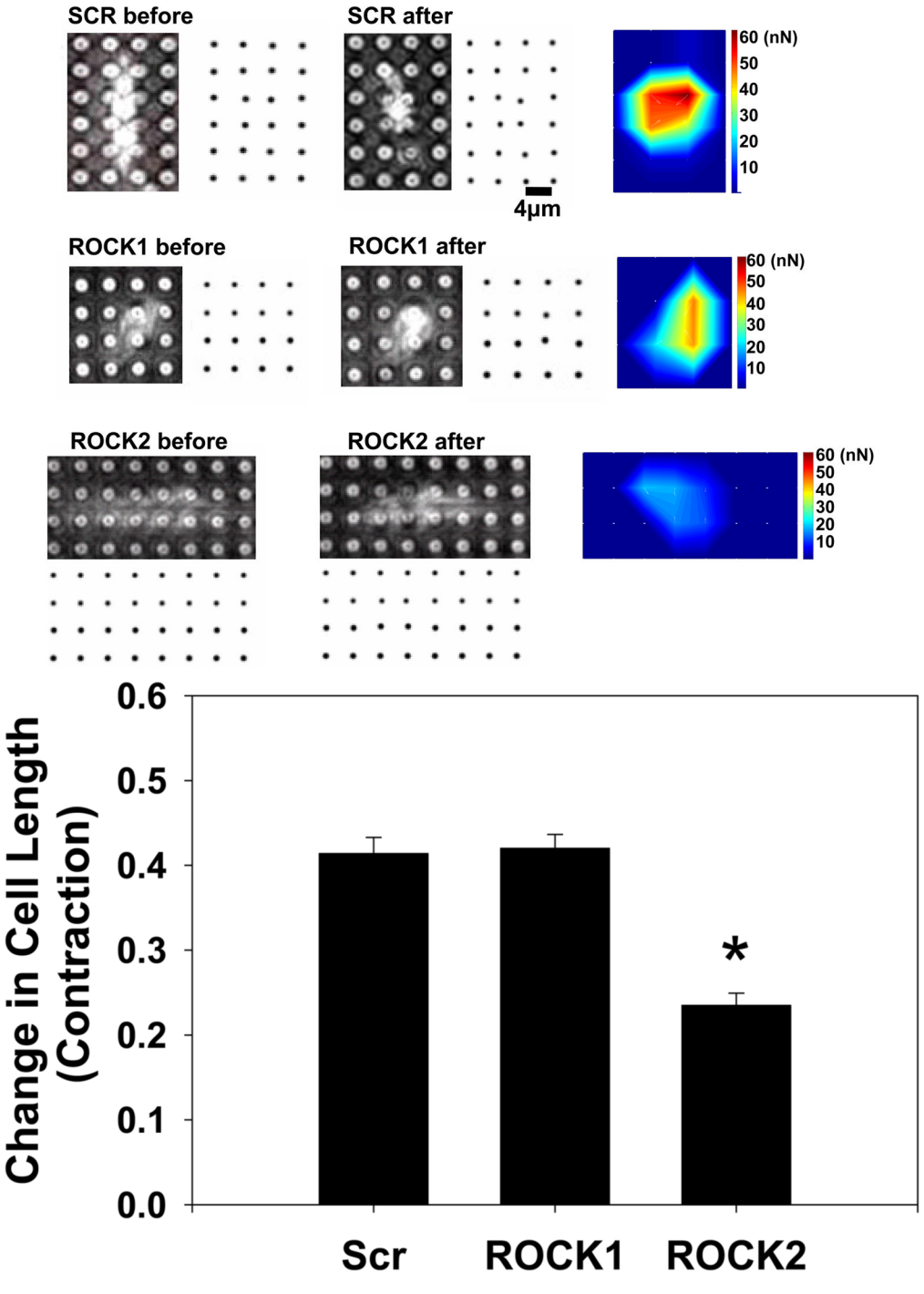

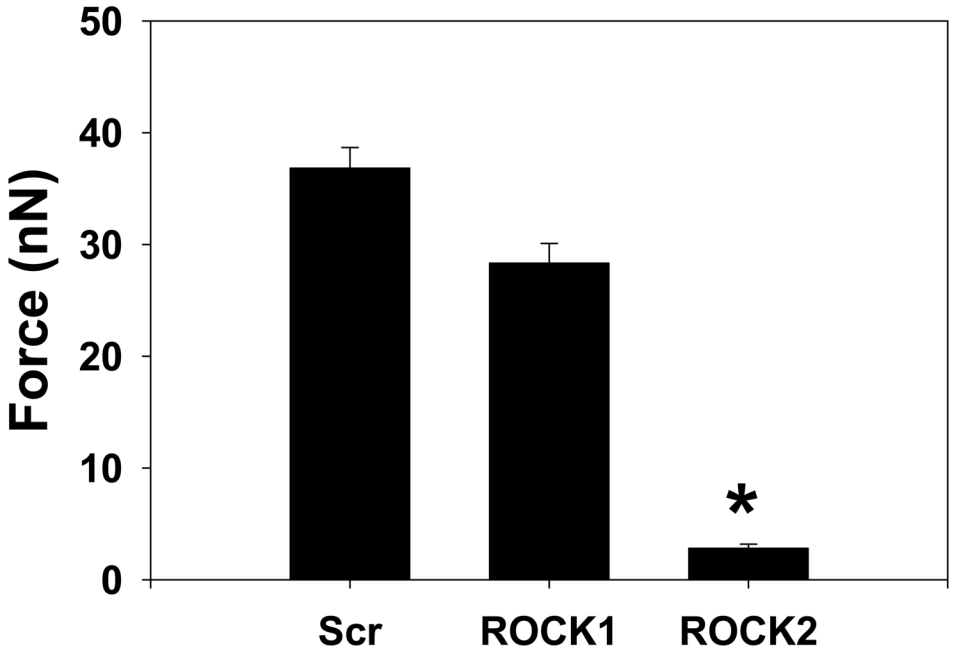

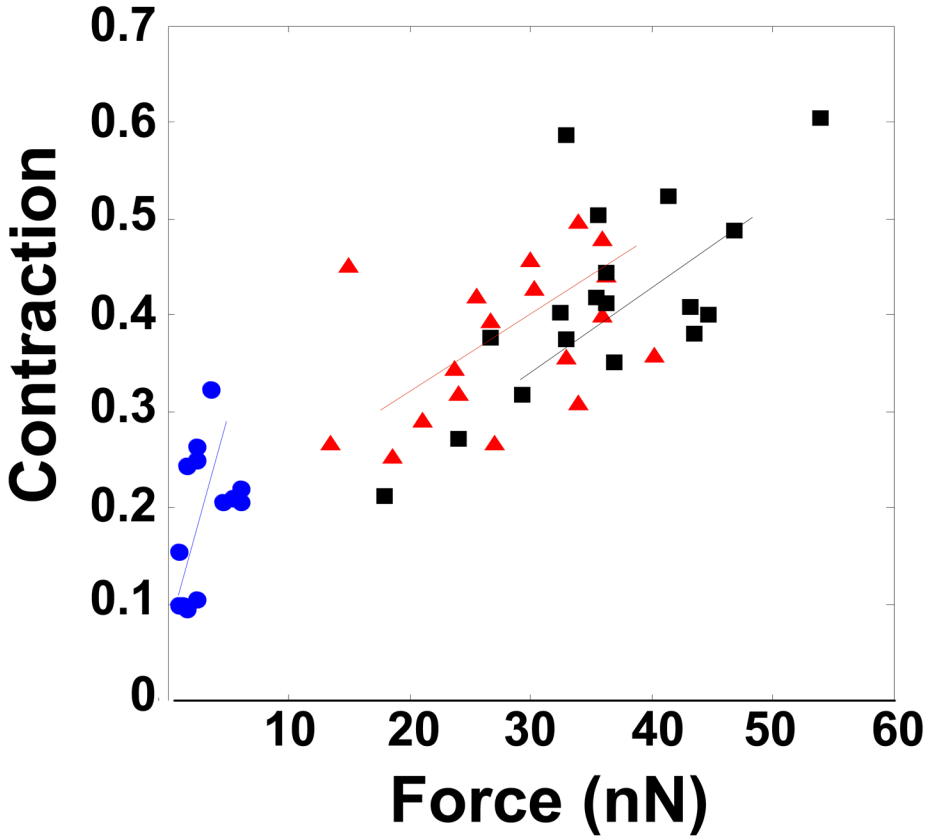

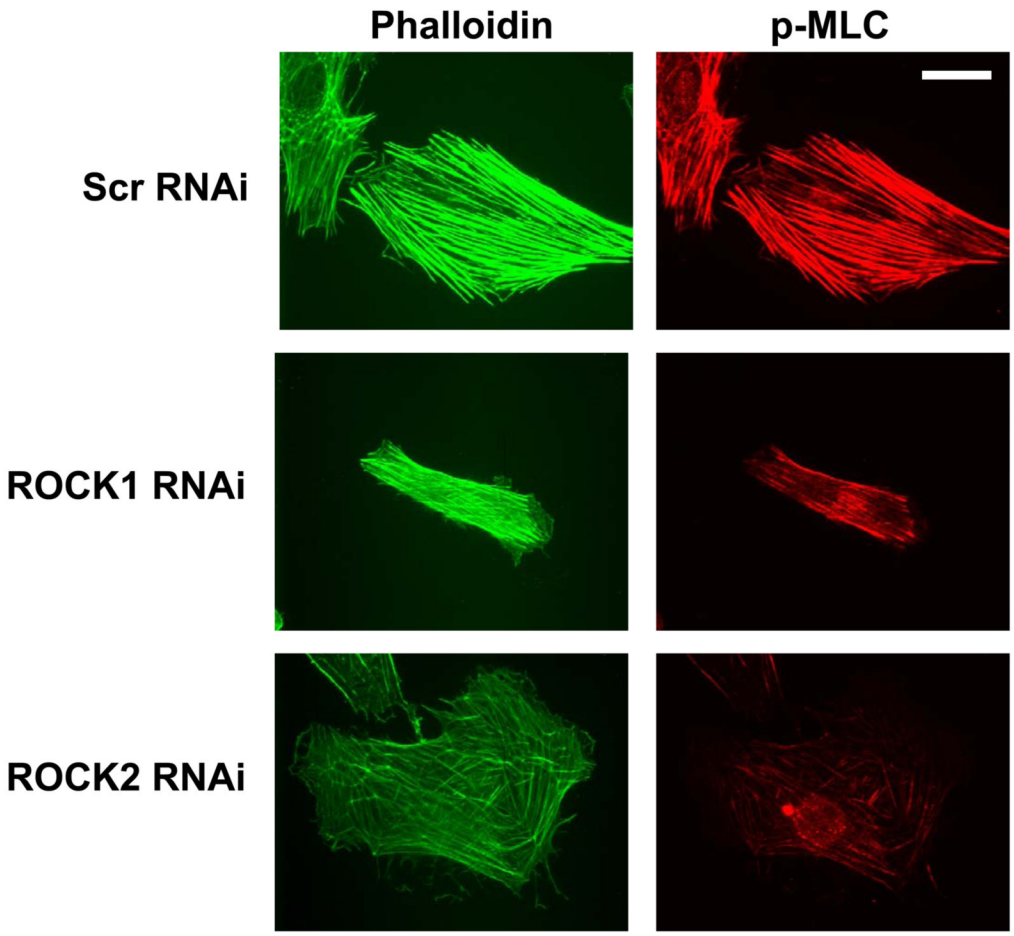

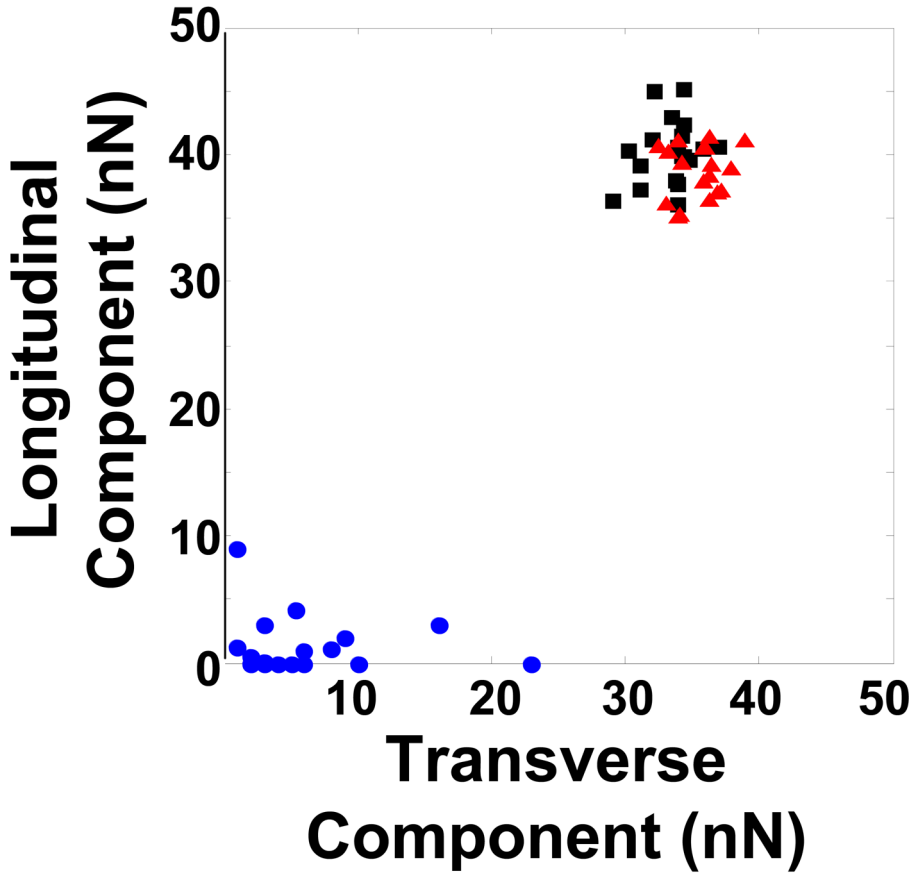

Figure 7. Contraction and Force Production in ROCK1 and ROCK2 silenced VSMCs

(A) Contractility and force production in representative scrambled negative control (Scr), ROCK1 and ROCK2 silenced primary rat aortic VSMCs. For each silencing condition, the phase-contrast image of the cell is shown before and 30 minutes after administration of 1μM LPA. Adjacent to the cell is the displacement map of the microfabricated posts. The displacement map was used to generate the force map shown to the far right of each image, as described in Methods. (B) Contraction, as measured by the change in cell length, in scrambled negative control (Scr), ROCK1 and ROCK2 silenced VSMCs treated with LPA, N=60, 69, 54 cells, respectively. (C) Force production in 20 scrambled negative control (Scr), ROCK1 and ROCK2 silenced cells treated with LPA. (D) Plot of force versus contraction for scrambled negative control (Scr, black squares), ROCK1 (red triangles) and ROCK2 (blue circles) silenced VSMCs. (E) Detail of scrambled negative control (Scr), ROCK1 and ROCK2 silenced unstimulated VSMCs labeled with phalloidin for actin filaments and phospho-MLC as in 5E. The scale bar is 30μm. (F) Plot of force direction analyzed in the longitudinal and transverse axes for scrambled negative control (black squares), ROCK1 (red triangles) and ROCK2 (blue circles) silenced LPA stimulated VSMCs. Force direction was determined by the direction in which the posts were bent and the average longitudinal and transverse components were plotted.